Observation of an Unusual Molecular Switching Device. The Position of One 1,2-Dimethylimidazole Switched "On" or "Off" the Rotation of the Other 1,2-Dimethylimidazole in *cis,cis,cis*-$Ru^{II}Cl_2(Me_2SO)_2$(1,2-dimethylimidazole)$_2$

Marian Iwamoto, Enzo Alessio,† and Luigi G. Marzilli*

Department of Chemistry, Emory University, Atlanta, Georgia 30322

Received August 11, 1995[⊗]

Some *cis,cis,cis*-$RuX_2(Me_2SO)_2$(1,2-Me_2Im)L complexes [L = 1,2-Me_2Im (1,2-dimethylimidazole) or Me_3Bzm (1,5,6-trimethylbenzimidazole), X = Cl or Br, and Me_2SO = S-bonded DMSO] have been synthesized and their rotamers studied in $CDCl_3$. From 2D NMR data, *cis,cis,cis*-$RuCl_2(Me_2SO)_2$(1,2-Me_2Im)(Me_3Bzm) has 1,2-Me_2Im in position "a" (*cis* to both Me_2SO's and *cis* to "b") and Me_3Bzm in position "b" (*trans* to one Me_2SO and *cis* to the other). There are two stable atropisomers [head-to-tail (HT, 84%) and head-to-head (HH, 16%), defining the aromatic H of Ru−N−C−H as head for both ligands]. Me_3Bzm has the same orientation in both atropisomers. In this orientation, the unfavorable interligand steric interactions of Me_3Bzm with the Me_2SO and 1,2-Me_2Im ligands appear to be countered by favorable electrostatic attraction between the $\delta+$ N_2CH moiety of Me_3Bzm and the $\delta-$ *cis* Cl ligands. The 1,2-Me_2Im lacks a $\delta+$ N_2CH group, and its orientation is dominated by steric effects of the 2-Me group. The NMR spectrum of *cis,cis,cis*-$RuCl_2(Me_2SO)_2$(1,2-Me_2Im)$_2$ is consistent with four rotamers in restricted rotation about both Ru−N bonds: two HH and two HT. 2D NMR techniques (NOESY and ROESY) afforded complete proton signal assignments. The ligand disposition could be assessed from the large chemical shift dispersion of some 1,2-Me_2Im ligand signals (Δ 0.86−1.52 ppm) arising from *cis*-1,2-Me_2Im shielding modulated by deshielding influences of the *cis* halides. The relative stability of the four rotamers correlates best with steric interactions between the 2-Me groups and the Me_2SO ligands. The most favorable conformer (46%) is the HH rotamer with both 2-Me groups pointing away from the Me_2SO ligands. The least favorable conformer (14%) was also HH, but the methyl groups in this case point toward the Me_2SO ligands. In the HT conformers of intermediate stability (∼20%), one 2-Me group is toward and the other is away from the Me_2SO ligands. The exchange cross-peaks in the 2D spectra are unusually informative about the dynamic processes in solution; the spectra provide evidence that the rotamers interchange in a definite pattern of succession. Thus, all conceivable exchange pathways are not available. 1,2-Me_2Im "b" can rotate regardless of the orientation of 1,2-Me_2Im "a". 1,2-Me_2Im "a" can rotate *only* when "b" has the orientation with its 2-Me group directed away from "a". Thus, 1,2-Me_2Im "b" can switch 1,2-Me_2Im "a" rotation on or off.

Introduction

The distribution of ligands among coordination positions of metal centers has been a primary focus of inorganic coordination chemists. However, less attention has been paid to the orientation of ligands with respect to other ligands. With the powerful structural methods now available, the elucidation of ligand orientation and of the factors that influence such orientation is now achievable. We are interested in orientation effects of nucleobases coordinated to metalloanticancer drugs via a single σ bond, since the consequent effect of orientation in DNA adducts may influence DNA structure and thus modulate anticancer activity. This interest has led us to investigate orientation effects in ligands that can serve as biological models but which are simpler than those normally found in biological systems.[1] The elucidation of ligand orientations in solution requires that rotation about the σ bonds be restricted.

The phenomenon of restricted rotation about metal−ligand σ bonds in simple coordination compounds has been studied in detail in a few square-planar complexes[2−13] but has seldom been investigated in complexes with 6 or higher coordination number.[1,14] Higher-coordinate inorganic stereodynamic systems typically studied involve fluxional isomerism in π-bound ligands or scrambling in carbonyl clusters.[15,16]

The strong interest in square-planar platinum(II) analogues of cisplatin (*cis*-$PtCl_2(NH_3)_2$) arises from their anticancer properties, whose mechanism of action is still under extensive investigation.[17] These drugs function by attacking nucleobases

† On leave from the Dipartimento di Scienze Chimiche, Università di Trieste, Trieste, Italy.

⊗ Abstract published in *Advance ACS Abstracts,* March 15, 1996.

(1) Marzilli, L. G.; Iwamoto, M.; Alessio, E.; Hansen, L.; Calligaris, M. *J. Am. Chem. Soc.* **1994**, *116*, 815.
(2) Lempers, E. L. M.; Bloemink, M. J.; Reedijk, J. *Inorg. Chem.* **1991**, *30*, 201.
(3) Sundquist, W. I.; Bancroft, D. P.; Lippard, S. J. *J. Am. Chem. Soc.* **1990**, *112*, 1590.
(4) Xu, Y.; Natile, G.; Intini, F. P.; Marzilli, L. G. *J. Am. Chem. Soc.* **1990**, *112*, 8177.
(5) Inagaki, K.; Dijt, F. J.; Lempers, E. L. M.; Reedijk, J. *Inorg. Chem.* **1988**, *27*, 382.
(6) Reily, M. D.; Marzilli, L. G. *J. Am. Chem. Soc.* **1986**, *108*, 6785.
(7) Coffindaffer, T. W.; Westler, W. M.; Rothwell, I. P. *Inorg. Chem.* **1985**, *24*, 4565.
(8) Reily, M. D.; Wilkowski, K.; Shinozuka, K.; Marzilli, L. G. *Inorg. Chem.* **1985**, *24*, 37.
(9) Marcelis, A. T. M.; Erkelens, C.; Reedijk, J. *Inorg. Chim. Acta* **1984**, *91*, 129.
(10) Marcelis, A. T. M.; van der Veer, J. L.; Zwetsloot, J. C. M.; Reedijk, J. *Inorg. Chim. Acta* **1983**, *78*, 195.
(11) Chisholm, M. H.; Folting, K.; Huffman, J. C.; Rothwell, I. P. *Organometallics* **1982**, *1*, 251.
(12) Bushweller, C. H.; Hoogasian, S.; English, A. D.; Miller, J. S.; Lourandos, M. Z. *Inorg. Chem.* **1981**, *20*, 3448.
(13) Cramer, R. E.; Dahlstrom, P. L. *J. Am. Chem. Soc.* **1979**, *101*, 3679.
(14) Alessio, E.; Calligaris, M.; Iwamoto, M.; Marzilli, L. G. Submitted.
(15) Perrin, C. L.; Dwyer, T. J. *Chem. Rev.* **1990**, *90*, 935.
(16) Orrell, K. G.; Sik, V. *Annu. Rep. NMR Spectrosc.* **1987**, *19*, 79.

0020-1669/96/1335-2384$12.00/0

in DNA, forming Pt−N σ bonds. The nucleobase ligands are lopsided, and *cis*-bis(guanine) adducts, models for the lesion normally found when *cis*-type Pt anticancer drugs bind to DNA, have HT (head-to-tail) or HH (head-to-head) atropisomers. On the NMR time scale, purine nucleobase complexes in solution normally exhibit free rotation about the Pt−N(nucleobase) σ bond, and atropisomers cannot be distinguished. However, Cramer[13] demonstrated in some Pt−guanosine complexes that the guanosine rotation rate was reduced when the other ligands were bulky. Cramer found two species of roughly equal population based on the observation of two G H8 signals and concluded that these were the two possible HT rotamers.[13] Although this interpretation was reasonable, the similarity in the signal intensity did not allow the assignment of the two H8 signals to a single HH species to be excluded. Later, Reily and Marzilli used ^{195}Pt NMR to establish the presence of two species in a related system, showing that two HT species of similar stabilities were present.[6] In a later study, Xu *et al.*[4] were able to stereochemically control atropisomerization in Pt−GMP complexes. With a C_2-symmetric *cis*-type Pt drug analogue, they were able to detect the four base H8 signals from the three possible atropisomers in slow chemical exchange at ambient temperature. In this system, the distribution of atropisomers was quite different, with one HT much more stable than the other HT atropisomer. Furthermore, an HH atropisomer was detected in solution for the first time.

Inorganic complexes with higher coordination number are more complicated and thus more difficult to study. Recently, we showed that *cis,cis,cis*-$RuCl_2(Me_2SO)_2(Me_3Bzm)_2$[1] [$Me_3Bzm$ = 1,5,6-trimethylbenzimidazole and Me_2SO = S-bonded dimethyl sulfoxide (DMSO)] exists as two rotamers of nearly equal stabilities. The ^{1}H NMR spectra indicated restricted rotation on the NMR time scale. The two rotamers interchange by a 180° rotation about only *one* of the two Ru−Me_3Bzm σ bonds, namely the Me_3Bzm *trans* to Cl.[14] We now report a detailed NMR study of another dynamic Ru octahedral complex, *cis*,-*cis,cis*-$RuCl_2(Me_2SO)_2(1,2\text{-}Me_2Im)_2$ (1,2-Me_2Im = 1,2-dimethylimidazole). The difference in bulk between two imidazole and two benzimidazole ligands has the potential of substantially changing the both the number and distribution of isomers. There is a possibility of slow rotation about *both* metal−nitrogen bonds instead of only one. *cis,cis,cis*-$RuCl_2(Me_2SO)_2$(1,2-Me_2Im)-(Me_3Bzm), a mixed-ligand derivative, was also studied.

We utilized NMR spectroscopy as our main tool for this investigation. Proton signals were assigned by using two-dimensional (2D) techniques such as exchange correlation spectroscopy (EXSY)[18−20] and rotating-frame Overhauser enhancement spectroscopy (ROESY).[21−23] Spectral data were also used to probe the dynamic behavior of the complexes.

This work was further stimulated by our interest in the chemistry of ruthenium−sulfoxide complexes.[24] These complexes have been shown to possess good antitumor properties.[25]

Experimental Section

Physical Measurements. NMR experiments were performed as described previously.[1] Elemental analyses were performed by Atlantic Microlabs, Atlanta, GA.

Reagents. Hydrated $RuCl_3$ was a loan from Johnson Matthey. DMSO and all the other solvents (Fisher) were used without further purification. All other reagents were from Aldrich. Deuterated solvents were purchased from Aldrich and Cambridge Isotope Laboratories.

Starting Materials. *cis*- and *trans*-$RuX_2(Me_2SO)_4$ (X = Cl, Br) were prepared by known methods.[26] Deuterated *cis*-$RuCl_2(Me_2SO)_4$ was obtained by dissolving the complex in warm DMSO-d_6 (0.5 g in 3 mL, 30 min); addition of acetone induced precipitation of the product. *cis,fac*-$RuCl_2(Me_2SO)_3(Me_3Bzm)$[14] was prepared as previously reported.

***cis,cis,cis*-$RuCl_2(Me_2SO)_2(1,2\text{-}Me_2Im)_2$ (1).** 1,2-Me_2Im (440 μL, 5 mmol) was added to a suspension of *cis*-$RuCl_2(Me_2SO)_4$ (1 g, 2 mmol) in absolute ethanol (60 mL). The magnetically stirred solution was heated at reflux for 1.5 h to give an orange solution that was concentrated *in vacuo* to ∼5 mL; after treatment with drops of hexane, the solution was refrigerated. The yellow precipitate that formed in 2 days was collected and rapidly washed with small amounts of cold ethanol and diethyl ether and vacuum-dried at 25 °C (yield: 0.6 g, 56%). The complex was recrystallized from acetone/DMSO mixtures (0.6 g of crude complex in 8 mL of acetone and 250 μL of DMSO) by addition of diethyl ether (yield: 60%). Anal. Calcd for $C_{14}H_{28}Cl_2N_4O_2RuS_2$ (MW 520.49): C, 32.30; H, 5.42; N, 10.76; S, 12.32; Cl, 13.62. Found: C, 32.47; H, 5.44; N, 10.70; S, 12.22; Cl, 13.56.

***cis,cis,cis*-$RuBr_2(Me_2SO)_2(1,2\text{-}Me_2Im)_2$ (2).** A procedure similar to that for **1** was adopted (after the reaction, ethanol was replaced with acetone in order to facilitate precipitation of the product). As in all syntheses of *all-cis* derivatives, a mixture of *cis*- and *trans*-$RuBr_2(Me_2SO)_4$ can be used as starting material. The complex was recrystallized from acetone/DMSO mixtures (0.54 g of crude complex in 6 mL of acetone and 150 μL of DMSO) by adding diethyl ether. The orange microcrystalline product was collected, washed with acetone and diethyl ether, and vacuum-dried at 25 °C (yield: 70%). Anal. Calcd for $C_{14}H_{28}Br_2N_4O_2RuS_2$ (MW 609.39): C, 27.59; H, 4.63; N, 9.19; S, 10.52; Br, 26.22. Found: C, 28.17; H, 4.81; N, 8.68; S, 10.78; Br, 26.57.

***cis,cis,cis*-$RuCl_2(Me_2SO)_2(Me_3Bzm)(1,2\text{-}Me_2Im)$ (3).** 1,2-Me_2Im (35 μL, 0.4 mmol) was added to a suspension of *cis,fac*-$RuCl_2(Me_2SO)_3(Me_3Bzm)$ (150 mg, 0.26 mmol) in absolute ethanol (10 mL). When heated at reflux for 1.5 h, the magnetically stirred suspension became a clear, deep yellow solution. The volume was reduced to ∼2 mL by rotary evaporation. Diethyl ether was added, and the solution was stored at 4 °C. Yellow microcrystals, formed within a few days, were collected, washed with cold ethanol and diethyl ether, and then vacuum-dried at 25 °C. Diethyl ether (∼2 mL) was added dropwise to a solution of the crude product (240 mg in 5 mL of acetone and 0.5 mL of DMSO). After refrigeration, more diethyl ether was gradually added to the solution until yellow crystals of the product slowly formed; these were collected and washed as described above (yield: 60%). Anal. Calcd for $C_{19}H_{32}Cl_2N_4O_2RuS_2$ (MW 584.60): C, 39.04; H, 5.52; N, 9.58; S, 10.97; Cl, 12.13. Found: C, 39.16; H, 5.54; N, 9.58; S, 11.06; Cl, 12.18.

NMR Spectroscopy. ^{1}H NMR experiments were performed either at 361.10 MHz on a GE NT-360 spectrometer or at 599.64 MHz on a GE GN-600 Omega spectrometer. Sample concentrations were ∼100 mM; solvents used include $CDCl_3$ and CD_2Cl_2. All spectra were referenced to TMS.

(a) 2D ^{1}H−^{1}H EXSY. The phase-sensitive proton 2D EXSY experiment[18−20] was performed on the GN-600 Omega at 25 °C. A 512 × 2048 data matrix was collected with 48 scans per t_1 increment. Each acquisition contained a 2-s relaxation delay, and the entire experiment was preceded by four dummy scans. A mixing time of 500 ms was implemented along with a 5555.56 Hz spectral window. Care was taken in optimizing the preacquisition-delay/dwell ratio in order to minimize B phase adjustment. The data were processed in a phase-sensitive absorption mode with Felix 1.1 or Felix 2.05 (Hare Research, Inc., Bothell, WA) on an SGI 4D/25 Personal Iris or Iris

(17) Sherman, S. E.; Lippard, S. J. *Chem. Rev.* **1987**, *87*, 1153.
(18) States, D. J.; Haberkorn, R. A.; Ruben, D. J. *J. Magn. Reson.* **1982**, *48*, 286.
(19) Kumar, A.; Ernst, R. R.; Wüthrich, K. *Biochem. Biophys. Res. Commun.* **1980**, *95*, 1.
(20) Jeener, J.; Meier, B. H.; Bachmann, P.; Ernst, R. R. *J. Chem. Phys.* **1979**, *71*, 4546.
(21) Griesinger, C.; Ernst, R. R. *J. Magn. Reson.* **1987**, *75*, 261.
(22) Bax, A.; Davis, D. G. *J. Magn. Reson.* **1985**, *63*, 207.
(23) Bothner-By, A. A.; Stephens, R. L.; Lee, J.-m.; Warren, C. D.; Jeanloz, R. W. *J. Am. Chem. Soc.* **1984**, *106*, 811.
(24) Alessio, E.; Sessanta o Santi, A.; Faleschini, P.; Calligaris, M.; Mestroni, G. *J. Chem. Soc., Dalton Trans.* **1994**, 1849.
(25) Mestroni, G.; Alessio, E.; Sava, G.; Pacor, S.; Coluccia, M.; Boccarelli, A. *Met.-Based Drugs* **1994**, *1*, 41.
(26) Alessio, E.; Mestroni, G.; Nardin, G.; Attia, W. M.; Calligaris, M.; Sava, G.; Zorzet, S. *Inorg. Chem.* **1988**, *27*, 4099.

Chart 1. Numbering Scheme and the Intraligand NOE Connectivity Path for the 1,2-Me_2Im Ligand

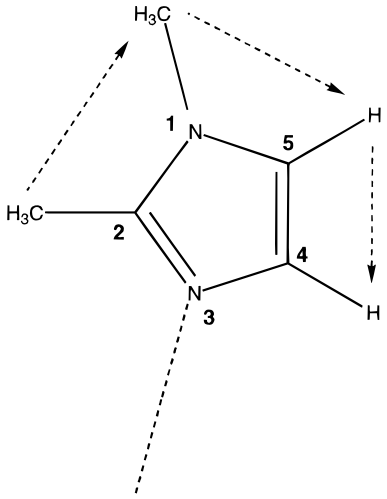

Chart 2. Labeling Scheme for the Octahedral Ru Complex Ligand Positions

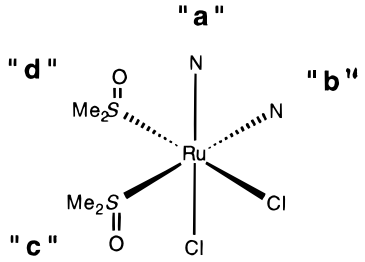

Indigo computer. An exponential multiplication with a line broadening of 3 Hz was applied to the t_2 dimension. The second dimension was zero-filled to 2048 data points, and a 45° shifted square sine bell filter was applied to the first 512 data points prior to Fourier transformation.

(b) 2D ^{1}H−^{1}H ROESY. The homonuclear hypercomplex 2D ^{1}H ROESY experiments[21−23] were performed on the GN-600 Omega spectrometer at 25 °C. Totals of 512 × 2048 data matrices were collected with 48−64 scans per t_1 increment. The spectrometer frequency was set off-center, downfield. An 8333.33 Hz window was used along with a spin lock field of 3571.43 Hz for **1** and 3030.30 Hz for **1** with DMSO-d_6. A 10 000 Hz window was used for **3** with a spin lock field of 3571.43 Hz. All spin locks were implemented with a 500-ms duration. A 2-s relaxation delay was incorporated prior to each scan, and the entire experiment was preceded by four dummy scans. Care was taken in optimizing the preacquisition-delay/dwell ratio in order to minimize B phase adjustment. The data were processed in a phase-sensitive absorption mode. The spectrum of **1** was processed in the t_2 dimension using an exponential multiplication with a line broadening of **1** Hz. The t_1 dimension was zero-filled to 2048 data points, and a Gaussian filter with a coefficient of 0.05 and line broadening of −20 Hz was applied. The spectrum of **1** with DMSO-d_6 was processed using a Gaussian filter with a coefficient of 0.1 and line broadening of −1 Hz in the t_2 dimension. The second dimension was zero-filled to 2048 data points, and a 75° shifted square sine bell filter was applied to the first 512 data points prior to Fourier transformation. The data in the first dimension of the spectrum of **3** were apodized with an exponential multiplication (line broadening of 1 Hz). The t_1 dimension was apodized with a 60° shifted square sine bell filter over the first 256 points. Data were zero-filled to 2048 data points.

Results and Discussion

In the absence of restricted rotation, the ^{1}H NMR spectrum of *cis,cis,cis*-$RuCl_2(Me_2SO)_2(1,2\text{-}Me_2Im)_2$ (**1**) (Charts 1 and 2) should have four aromatic signals (two from each 1,2-Me_2Im ligand) and eight methyl signals (two from each 1,2-Me_2Im ligand and two from each Me_2SO ligand). The observed spectrum of **1** in $CDCl_3$ [16 aromatic signals between 6.4 and 8.0 ppm (Figure 1) and 29 resolved resonances in the methyl region] was consistent with the presence of four rotamers. Slow interconversion on the NMR time scale was found in ROESY and NOESY experiments, confirming that the species are rotamers and not a mixture of geometric isomers.

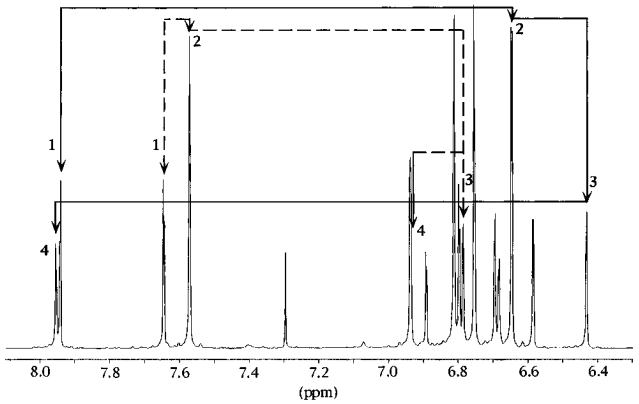

Figure 1. Downfield region of the 1D ^{1}H NMR spectrum of *cis,cis,cis*-$RuCl_2(Me_2SO)_2(1,2\text{-}Me_2Im)_2$ (**1**). Arrows indicate the four rotamers of H4 and their conversion pathway: (− −) 1,2-Me_2Im "a"; (—) 1,2-Me_2Im "b".

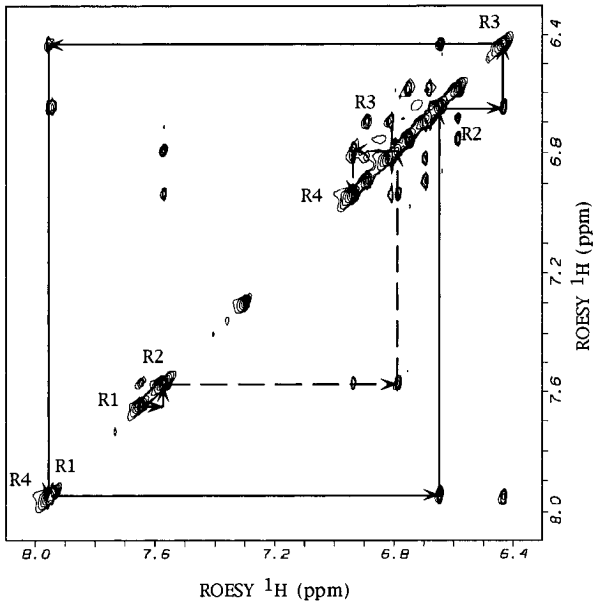

Figure 2. Downfield region of the ^{1}H−^{1}H ROESY spectrum at 25 °C of *cis,cis,cis*-$RuCl_2(Me_2SO)_2(1,2\text{-}Me_2Im)_2$ (**1**) depicting the exchange cross-peaks (*i.e.*, negative cut) and pathways. The H4 connectivities of the four rotamers are shown for 1,2-Me_2Im "a" (− −) and 1,2-Me_2Im "b" (—).

Close examination of the downfield region of the ROESY spectrum (Figure 2) revealed definite exchange pathways for H4 and H5 and identified four rotamers (**R1**-**R4**) in slow exchange. Peak integration of the 1D spectrum gave an approximate **R1**:**R2**:**R3**:**R4** ratio of 1.5:3.4:1.5:1.

The proton signals were completely assigned by the following procedure (peak attribution was done mainly on the most abundant rotamer): (i) Synthesis of the complex with DMSO-d_6 allowed identification of the Me_2SO methyl peaks. (ii) H5 and 1-Me were assigned because of their strong intraligand NOE; H4 and 2-Me were assigned through H5−H4 and 1-Me-2-Me cross-peaks (Chart 1). (iii) Me_2SO methyl signals belonging to the same ligand have strong NOE cross-peaks. (iv) Assignments of signals to particular rotamers were made on

Table 1. ^{1}H Chemical Shifts (ppm) of *cis,cis,cis*-$RuCl_2(Me_2SO)_2(1,2\text{-}Me_2Im)_2$ (**1**) (100 mM in $CDCl_3$)[a]

	R1	R2	R3	R4
		1,2-Me_2Im "a"		
H4	7.64	7.57	6.78	6.93
H5	6.80	6.75	6.59	6.68
1-Me	3.55	3.50	3.60	3.63
2-Me	2.05	2.00	2.73	2.76
		1,2-Me_2Im "b"		
H4	7.94	6.64	6.43	7.95
H5	6.94	6.81	6.69	6.89
1-Me	3.65	3.68	3.64	3.59
2-Me	1.95	3.01	3.01	1.81
		Me_2SO "c"		
	3.41	3.36	3.45	3.48
	2.91	2.93	2.92	2.93
		Me_2SO "d"		
	3.74	3.70	3.60	3.68
	2.83	2.86	2.81	2.78

the basis of peak intensities (all methyl peaks belonging to the same rotamer have the same intensity) and some exchange peaks in the ROESY spectrum. (v) Attribution of ligand position, *i.e*. which ligand is in position "a" (*cis* to both Me_2SO's) and which in position "b" (*cis* to both Cl's) (Chart 2), was accomplished through the interligand NOEs; H4 of 1,2-Me_2Im "a" has NOE peaks to both Me_2SO's, while H4 of 1,2-Me_2Im "b" has an NOE with only one Me_2SO, "d".

The exchange peaks allowed us to correlate a given type of signal for all four rotamers, although all exchange pathways were not present (*cf*. Figure 2). For example, the H4 signal of 1,2-Me_2Im "b" at 7.94 ppm (intermediate abundance—**R1**) has one exchange cross-peak to the H4 signal at 6.64 ppm (most abundant—**R2**). The 6.64 ppm signal, in turn, has another exchange cross-peak to the H4 signal at 6.43 ppm (intermediate abundance—**R3**). The 6.43 ppm signal has an exchange cross-peak to the downfield H4 signal at 7.95 ppm (least abundant—**R4**). In addition, the 7.95 ppm signal has a weak cross-peak to the 6.64 ppm signal. A similar pattern of H4 exchange peaks is present for ligand "a". The downfield H4 signal at 7.64 ppm (intermediate abundance—**R1**) has only one exchange cross-peak; this is to the H4 signal at 7.57 ppm (most abundant—**R2**). The 7.57 ppm signal has another exchange cross-peak to the 6.78 ppm signal (intermediate abundance—**R3**). This H4 signal in turn has a cross-peak to the 6.93 ppm signal (least abundant—**R4**). H5 signals for 1,2-Me_2Im "a" and "b" are linked in a similar manner. All of the signals were thus readily assigned to a distinct rotamer (Table 1).

For the H4 and other signals, two of the rotamers have two strong exchange peaks, while the other two rotamers have only one strong exchange peak (Figure 2). These exchange peaks suggest that there is a definite pattern of progression between the four rotamers and that each rotamer cannot randomly interconvert into another form. The following exchange path among the rotamers was indicated by these peaks:

$$\mathbf{R1} \Leftrightarrow \mathbf{R2} \Leftrightarrow \mathbf{R3} \Leftrightarrow \mathbf{R4}$$

There is a weak cross-peak between the H4 "a" signals of **R2** and **R4**, consistent with two sequential exchanges.

The following hypotheses were assessed to determine if they could be used to explain the nature of the four rotamers and their interconversion pathway: (i) one 1,2-Me_2Im is in slow exchange among four positions in progression (possibly 90° from each other) while the other one either is in a fixed position or is in fast rotation or (ii) both 1,2-Me_2Im ligands are independently flipping (probably by ~180°). Only the latter hypothesis agrees with the unusual chemical shift changes between the rotamers. There are large changes in chemical shift for H4 "b" between **R1** and **R2** and between **R3** and **R4**, suggesting that 1,2-Me_2Im "b" flips between **R1** and **R2** and between **R3** and **R4**. In contrast, there is a large change in chemical shift for H4 "a" between **R2** and **R3** and between **R1** and **R4**. Although there is also likely to be a flipped orientation for 1,2-Me_2Im "a" between these two pairs, there are no exchange peaks between **R1** and **R4**.

We now address the question of the orientations of the 1,2-Me_2Im ligands in these rotamers. Chart 3 and Figure 3 are consistent with both the chemical shift data and the relative abundance of the rotamers. **R2** and **R4** are HH atropisomers and **R1** and **R3** are HT atropisomers, (the head being defined as the H4 end of the ligand). As found for the Me_3Bzm analogue of **1**,[1,14] ligand "b" has the most downfield signals (H4 in two of the rotamers, **R1** and **R4**); moreover, these two signals undergo a clear downfield shift in the dibromo analogue (**2**) (to 8.22 and 8.20 ppm). This shift suggests that H4 of "b" in **R1** and **R4** points toward the two *cis* halogens.[14,27,28]

For both ligands "a" and "b", a downfield shift of H4 always corresponds to an upfield shift of 2-Me and vice versa. The largest factors affecting the chemical shifts are the shielding cones of the two imidazole rings. When a group is directed toward the halides, its signal exhibits a slight downfield shift caused by the halide. In the case of **R1** (and **R4**), 2-Me "b" falls into the shielding cone of "a" while 2-Me "a" falls into the shielding cone of "b"in **R1** (and **R2**) (cf. Figure 3). Since it points toward the halogens in **R1** (and also **R2**), 2-Me "a" is slightly more downfield shifted than 2-Me "b" in **R1** and **R4**. Using this type of reasoning, all the 2-Me and H4 signals can be analyzed: for example, the shielding effects of 1,2-Me_2Im "b" on H4 "a" in **R3** and **R4** are countered by the halide effect compared with H4 "b" in **R2** and **R3**.

NOEs present in the ROESY spectrum are consistent with the base orientations derived from the shifts. *For **R1***, both 2-Me's are close and both H4's are far apart. H4 "a" is in proximity to the Me_2SO ligands. We find a strong NOE between the two 2-Me signals and no evident NOE between the H4's. The H4 "a" signal has cross-peaks to two Me_2SO signals, 2.91 and 3.74 ppm, assigned to ligands "c" and "d", respectively. *For **R2***, 2-Me "a" is close to H4 "b" and H4 "a" is far from 2-Me "b". ROESY data reveal a strong NOE between the 2-Me "a" and H4 "b". NOEs are present between H4 "a" and the signals at 2.93, 3.70, and 2.86 ppm, signals from the methyl groups of ligands "c" and "d", consistent with H4 "a" being close to the Me_2SO ligands. *For **R3***, we would expect to see NOEs between the two H4 signals and no NOE between the signals of the more distant 2-Me's. A medium-intensity cross-peak is present between the H4 signals. No clear NOE is evident between the two 2-Me signals. NOEs should also be present between 2-Me "a" and the *cis*-Me_2SO ligands. An NOE is present between the signals at 2.73 ppm (2-Me "a") and 3.60 ppm (Me_2SO "d"). Finally, *for **R4***, H4 "a" is in close proximity to 2-Me "b". As expected, an NOE is present between these two signals (6.93 and 1.81 ppm); in addition, no NOE is seen between the signals of the well-separated 2-Me "a" and H4 "b", as expected.

We believe that the stability of the rotamers is determined mainly by the steric interactions between the 2-Me groups and the two Me_2SO ligands. **R4** is the least stable of the four, as the 2-Me groups of the two ligands are both pointing toward

(27) Barnes, J. R.; Goodfellow, R. J. *J. Chem. Res., Miniprint* **1979**, 4301.
(28) Barnes, J. R.; Goggin, P. L.; Goodfellow, R. J. *J. Chem. Res., Miniprint* **1979**, 1610.

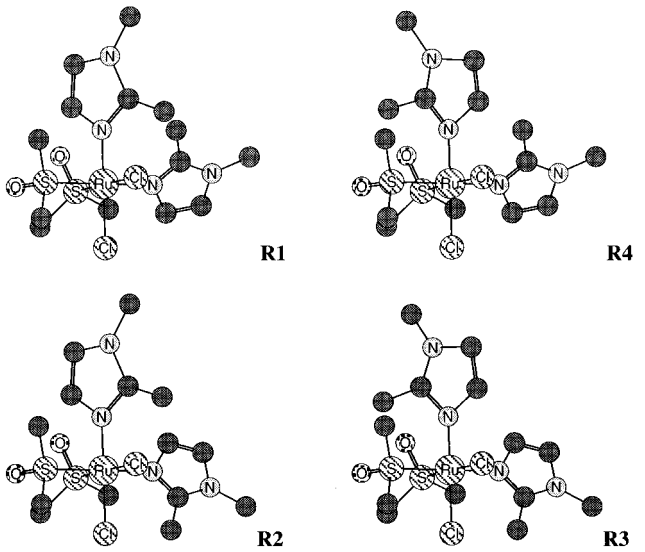

Figure 3. Perspective drawings for **1** (**R1**−**R4**). The proposed orientation of the ligands is based on proton chemical shifts of **1** and the crystal structure of *cis,cis,cis*-$RuCl_2(Me_2SO)_2(Me_3Bzm)_2$.[1]

Chart 3. Proposed Ligand Orientations in the Four Rotamers of **1**[a]

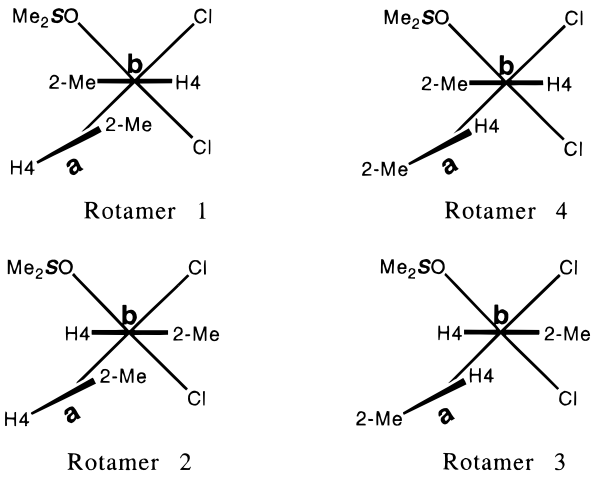

[a] "b" is above the plane of the paper, and for clarity, Me_2SO "c" is not shown.

Me_2SO ligands, while **R2** is the most stable, since the two 2-Me groups are far from the Me_2SO ligands (Chart 3 and Figure 3). The two HT rotamers, **R1** and **R3**, have comparable steric interactions and stability.

Another conclusion that can be drawn is that position "a" of **1** is the most hindered, in agreement with "a" being *cis* to two Me_2SO ligands, while "b" is *cis* to only one. In fact, while in all rotamers 1,2-Me_2Im "b" is always free to flip back and forth, 1,2-Me_2Im "a" cannot flip back and forth from **R1** to **R4** (when the 2-Me of "b" points toward the "a" ligand), since there are no exchange peaks between the two. Examination of models suggests that rotation of "a" from **R2** to **R3** is relatively free since there are no steric interactions with 2-Me "b". The cross-peak between **R4** and **R2** suggests that, in **R4**, rotation of "a" and "b" can occur in progression during the mixing time in the NMR experiments. In platinum complexes,[4] exchange peaks attributable to two sequential rotations occurring during the mixing time are commonly observed.

For *cis,cis,cis*-$RuCl_2(Me_2SO)_2(Me_3Bzm)$(1,2-$Me_2$Im) (**3**), five aromatic signals and nine ^{1}H NMR methyl signals are expected for a single rotamer; however, twice the number of signals were found, suggesting the presence of only two rotamers. The

Table 2. ^{1}H Chemical Shifts (ppm) of *cis,cis,cis*-$RuCl_2(Me_2SO)_2(Me_3Bzm)$(1,2-$Me_2$Im) (**3**) in $CDCl_3$[a]

	R1	**R2**		**R1**	**R2**
		1,2-Me_2Im "a"			
H4	7.78	6.56	1-Me	3.34	3.64
H5	6.84	6.39	2-Me	1.51	2.86
		Me_3Bzm "b"			
B2H	8.81	8.84	$B10H_3$	2.11	2.10
B4H	6.56	6.54	$B11H_3$	2.37	2.34
B7H	7.21	7.16	$B12H_3$	3.92	3.90
		Me_2SO "c"			
CH_3(1)	3.47	3.53	CH_3(2)	3.01	3.02
		Me_2SO "d"			
CH_3(1)	3.73	3.67	CH_3(2)	2.67	2.62

[a] See Chart 1 for 1,2-Me_2Im notation, Chart 4 for Me_3Bzm notation, and Chart 2 for ligand positions. **R1**, HT (84% abundant); **R2**, HH (16% abundant).

Chart 4. Numbering Scheme and the Intraligand NOE Connectivity Path for the Me_3Bzm Ligand[a]

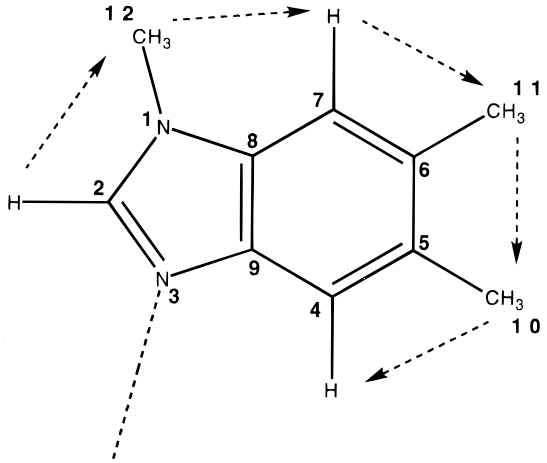

[a] The carbons are designated "B" (for benzimidazole) in the references to NMR results in the text.

rotamers were present in a ∼5:1 ratio (**R1**:**R2**). All ^{1}H signal assignments and ligand dispositions (Table 2) were determined from a ROESY spectrum in which intra- and interligand NOEs were evident. The ROESY spectrum also revealed exchange peaks between the two sets of rotamer peaks. An assignment strategy similar to that for **1** was followed. The doublet at 6.84 ppm has a very strong NOE to the methyl signal at 3.34 ppm, designating these two signals as H5 and 1-Me, respectively. The H5 signal has a strong NOE to the doublet at 7.78 ppm, assigning it to H4; the 1-Me signal has a strong NOE to the 1.51 ppm signal, distinguishing it as 2-Me. For the Me_3Bzm ligand, the NOE path shown in Chart 4 was followed. Of the remaining methyl signals, the downfield one at 3.92 ppm was assumed to be the *N*-methyl ($B12H_3$) signal. This signal has NOEs to B2H and B7H, respectively. NOEs from B7H around the six-membered ring give the remaining signal assignments for $B10H_3$, $B11H_3$, and B4H.

Ligand dispositions (Chart 2) for **3** were assessed from interligand NOEs between the L and Me_2SO signals. NOEs are present between signals from 1,2-Me_2Im to both Me_2SO ligands, whereas signals from Me_3Bzm have NOEs to only one Me_2SO. This pattern of NOEs suggests that 1,2-Me_2Im is in the "a" position, *cis* to both Me_2SO's, and Me_3Bzm is in the "b" position, *cis* to only one Me_2SO (Chart 5).

From ^{1}H chemical shift analyses of **3**, we believe that the two rotamers are products of a slow rotation of the 1,2-Me_2Im ligand (large shift changes between rotamers) while the Me_3-

Chart 5. Proposed Ligand Orientations in the Two Rotamers of **3**[a]

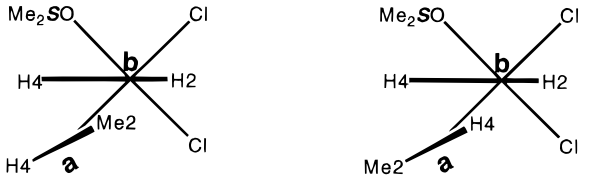

[a] See Chart 1 for 1,2-Me_2Im notation and Chart 2 for ligand positions.

Bzm ligand remains static (essentially no shift between rotamers). In an analog of **3**, *cis*,*cis*,*cis*-$RuCl_2(Me_2SO)_2$(py)(Me_3-Bzm) (py = pyridine), the py occupies the "a" position,[14] and the Me_3Bzm B2H points toward the halides (comparable B2H chemical shifts are found in the analogous complexes). The shifts also provide information about which rotamers are present. The major conformer (**R1**) has a HT structure in which the 1,2-Me_2Im H4 is oriented away from the halides (Chart 5). The minor conformer (**R2**) has a HH structure in which the 1,2-Me_2Im H4 is toward the halides. For **R1**, the greater upfield shift of 2-Me compared to that of **1** is caused by the larger shielding by Me_3Bzm, which has both five- and six-membered rings causing shielding. The proximity of the 2-Me to one *cis* halide, which in **R1** and **R2** of **1** modulated the upfield shift of 2-Me, may also have a modulating effect here, but this is difficult to assess. The H4 signal of 1,2-Me_2Im in **R2** is shifted upfield due to the shielding effects of Me_3Bzm.

NOEs present in the ROESY spectrum are consistent with **R1** HT and **R2** HH conformations (Chart 5). In **R1** 2-Me "a" is close to both B4H "b" and B2H "b". H4 "a", in contrast, is far from B2H "b" but close to the Me_2SO ligands. As expected for **R1**, NOEs are present between 2-Me "a" and B4H and B2H of ligand "b", while no NOE is evident between H4 "a" and B2H "b". The H4 "a" signal has cross-peaks to three Me_2SO signals, 3.47, 3.01, and 3.73 ppm, of ligands "c" and "d". In **R2**, H4 "a" is close to B2H "b"; 2-Me "a" is far from B2H "b". ROESY data reveal a weak NOE between the signals of H4 "a" and B2H "b". Other features consistent with the **R2** rotamer are as follows: no NOE present between 2-Me "a" and B2H "b"; an extremely weak NOE between 2-Me "a" and B4H "b"; and an NOE between 2-Me "a" and the signal at 3.67 ppm, a signal from the methyl group of Me_2SO "d".

For both **1** and **3**, it is clear that having the 2-Me group of the 1,2-Me_2Im pointing away from the Me_2SO ligands is favorable, and the conformers that minimize the steric interaction between the 2-Me and the Me_2SO ligands are favored regardless of whether position "a" or "b" is considered. In contrast, in **3** and in the two other Me_3Bzm complexes[1,14] with Me_3Bzm in position "b", the Me_3Bzm B2H is oriented toward the halides, and thus the bulky six-membered ring of Me_3Bzm has unfavorable steric interactions with the Me_2SO ligands. The fixed position of "b" likely results from the electrostatic interactions between B2H and the *cis* halides.[14] This finding is supported by the structural features of Me_3Bzm "a" in *cis*,*cis*,*cis*-$RuCl_2(Me_2SO)_2(Me_3Bzm)_2$.[1] The HH atropisomer of this complex can be crystallized, and distortions around the Ru−N−C angles of Me_3Bzm "a" clearly indicate steric hindrance. Nevertheless, the solution data show that this HH rotamer is comparable in stability to the HT rotamer. This ~1:1 ratio contrasts with the 5:1 ratio of **3**. H4 of 1,2-Me_2Im is likely to be less acidic than B2H, and the 2-Me group and the six-membered ring of Me_3Bzm are both bulky. Thus, only two rotamers are stable for **3**, whereas four rotamers can be observed with **1**.

Conclusions

NMR evidence has demonstrated restricted rotation in two six-coordinate Ru coordination complexes containing 1,2-Me_2-Im. In **1**, four rotamers were observed. The population pattern of the four rotamers is determined by the steric nature of the coordinated ligands. In **R2**, the most stable rotamer, the 1,2-Me_2Im ligands are arranged in a HH manner with the 2-Me groups pointing away from the Me_2SO ligands. This type of conformation is the least sterically demanding. The least stable conformer, **R4**, also has a HH arrangement of the nitrogen ligands, but in this case the 2-Me groups point toward the Me_2SO ligands. The HT arrangements of **R1** and **R3** are of comparable intermediate stability.

For the mixed-ligand complex, **3**, two rotamers are present in a 5:1 ratio. NMR spectra indicate slow rotation of the 1,2-Me_2Im ligand, while the bulkier Me_3Bzm ligand remains static. The populations of the two rotamers are governed by steric influences of the 1,2-Me_2Im methyl groups. Due to steric and electrostatic influences, the Me_3Bzm ligand remains static.

In the case of **1**, an interesting dynamic system was discovered, in which the rotation of ligands "a" and "b" follows a definite succession pattern: HT ⇔ HH ⇔ HT ⇔ HH (**R1**, **R2**, **R3**, and **R4**, respectively). 1,2-Me_2Im "a" is in the most hindered position and can flip back and forth only when the 2-Me group of ligand "b" points away from 1,2-Me_2Im "a" (*i.e.* toward the chloride ligands). Consequently, **R1** and **R4** cannot interconvert because of the orientation of 1,2-Me_2Im "b". Thus, in this study directed at understanding mutual interactions of heterocyclic ligands, we have discovered a simple molecular switching device. Of course, we have no way of controlling the switch. It is conceivable that related systems could be devised in which the orientations are controlled either photo- or electrochemically. For example, since the orientation seems to be influenced by electrostatic attraction, a change in oxidation state of the metal or (better) the ligand could be one means of controlling the switch.

Acknowledgment. We thank the NIH (Grant GM 29222) for support, NATO for a fellowship to E.A., and Johnson Matthey for a loan of $RuCl_3$. We also thank the NIH and NSF for supporting the purchase of instruments.

IC951063Z